Energy 275 (2023) 127458

Contents lists available at ScienceDirect

Energy

journal homepage: www.elsevier.com/locate/energy

Research on the new combustion chamber design to operate with low methane number fuels in an internal combustion engine with pre-chamber

Ander Ruiz Zardoya [a,d], Iñaki Loroño Lucena [b], Iñigo Oregui Bengoetxea [c], José A. Orosa [a,*]

[a] Universidade da Coruña, Department of N. S. and Marine Engineering, Paseo de Ronda, 51, 15011, A Coruña, Spain
[b] UPV/EHU, Departamento de Ciencias y Técnicas de la Navegación, Máquinas y Construcciones Navales, Escuela de Ingeniería de Bilbao (Edificio Portugalete), María Díaz de Haro, 68, 48920, Portugalete, Spain
[c] Guascor Energy Engines R&D, Department of Thermal Engines, Leonardo Da Vinci Kalea, 12, Vitoria-Gasteiz, 01510, Álava, Spain
[d] Guascor Energy SAU, Project Management and After Sales, Barrio Oikia, 44, Zumaia, 20750, Gipuzkoa, Spain

ARTICLE INFO

Handling Editor: Wojciech Stanek

Keywords:
Associated petroleum gas (APG)
Internal combustion engine
Low methane number

ABSTRACT

Gas flaring is the burning process of unwanted raw natural gas (NG) that cannot be processed during the oil and gas extraction and process operations. This research work aims to continue with the experimental prototyping and validation of a combustion chamber configuration to run low methane number (MN) fuels down to 35 with a 2 MW natural gas internal combustion engine (ICE) with a fuelled pre-chamber. As opposed to solutions available in the market for the aforementioned type of engines which are linked to huge power losses, the goal is not only to define a methodology to modify them to run those fuels consistently but also to achieve it with a minimum power and efficiency loss. The experiments conducted on a 175 kW single cylinder engine (SCE) in Guascor Energy's facilities, with a preliminary engine configuration, showed efficiency and output power loss when using low methane number gases. However, power losses were improved by 27.98% as compared with the previous work's results demonstrating the feasibility of the proposed technology. In particular, the highest losses were detected with a 35 methane number fuel, where the break mean effective pressure (BMEP) or output power reduction was 25.32% while efficiency losses reached values of 18.02%.

1. Introduction

Gas flaring is the burning process of unwanted raw natural gas associated with oil extraction. During the extraction process, a variable quantity of associated petroleum gas is found in the reservoir together with oil which is burnt or released into the atmosphere through a flare [1,2].

Nonetheless, part of the treated natural gas is frequently used for covering the site demands, while the unused natural gas is processed, sold or reinjected. Only when it is not possible to sell or process it the natural gas in excess is flared [3].

Researchers are working on alternatives to reduce flaring and ultimately reducing emissions and monetizing a by-product. Nevertheless, it is complex to find a solution that presents efficiency and economic feasibility.

The alternative that will be analysed herein underlines the power and heat generation burning flare gas in an internal combustion engine. In fact, there is a big market niche [4] for Combined Heat and Power (CHP) applications in plants where small quantities of APG are extracted [5] or just when it is not possible to sell it due to lack of infrastructure.

Different reviews regarding power generation technologies that may be subject to use APG [6] evidenced that Internal Combustion Engines (ICEs) have better economic indicators than the rest of the technologies. Some other studies focused on analysing the economic feasibility of different alternatives [7] concluded that feasibility was a function of the flow and composition of the available gas, highlighting a special interest in ICEs in flows below 10.000 m^3.

Amidst ICE advantages, one of the main characteristic of these engines relies on the wide range of power outputs available (from few kW to 15 MW). Furthermore, they are usually sold in a modular construction installing units of reduced power. This permits high thermal efficiency together with a high flexibility, as partial loads caused by the flow changes could be eliminated. Moreover, this configuration allows the reutilisation of the engines in different plants which is especially

* Corresponding author.
E-mail addresses: ander.ruiz@guascor-energy.com (A.R. Zardoya), inaki.lorono@ehu.eus (I.L. Lucena), inigooregui@gmail.com (I.O. Bengoetxea), jose.antonio.orosa@udc.es (J.A. Orosa).

https://doi.org/10.1016/j.energy.2023.127458
Received 3 August 2022; Received in revised form 6 March 2023; Accepted 5 April 2023
Available online 6 April 2023

interesting since the amount of APG reduces as the time goes by in the oilfields.

From an economic perspective, a profitability analysis was carried out in an oil field in Shandong province in China which demonstrated that a net benefit of about 28.539,00€ per engine could be achieved annually by installing an ICE. Further to it, when environmental benefits including health benefit and low-carbon benefit were included in the model, the annual benefits of a single equipment could amount to values up to 131.823,00€ of net benefit per year. Thus, by means of this study it is concluded that the application of CHP in oil extraction sites is economically profitable [8]. Another study in the field suggests the high profitability of using ICEs in oil fields. In particular, Vazim et al. point out that a power generation plant using ICEs at Yuzhno-Cheremshanskoe oil field has a demonstrated cost effectiveness over 75% with a shorter payback than two years, with total annual savings that amount to 857.737,77€ per year [11].

As far as emissions are concerned, past investigations exposed that generating power from well-head gas leads to a considerable diminution in SO_x and CO emissions. As ICEs present lower emissions than gas turbines the interest in using ICEs was again underlined [10].

However, it is remarkable that the APG is a low methane number gas as a consequence of the high content of heavy hydrocarbons in its composition. This fact increases the knocking tendency of the fuel limiting the knocking margin and ultimately reducing the output power and thermal efficiency [2].

Standard natural gas internal combustion engines are designed to operate with fuels with a methane number higher than 65. Thus, with the objective of avoiding knocking issues, technical modifications must be done to the engine so that low MN fuels are burnt in a profitable a safe manner. Those modifications were discussed by Ruiz et al. [11] and are summarized in Table 1.

Engine modifications to burn low methane number fuels have been of interest to researchers in the last years [12]. Engine modifications have been proposed such as using alternative fuels [13] or an E-Pilot injection together with a large squish piston [14], both showing an improvement in the efficiency and CH_4 emissions. Additionally, other investigations proposed mathematical methods to optimise the performance of internal combustion engines with new fuel tests [15] considering different technical and economical parameters [16,17].

During the present paper an alternative is presented to convert a natural gas engine with an active pre-chamber system to burn gas with a low methane number up to values of 35 which would cover any kind of APG. To date, there are not gas engines with an active pre-chamber technology available in the market to burn fuels around MN35. They generally need to be derrated and work with higher MN fuels. Thus, the present work offers a methodology to convert those natural gas engines to run with such a demanding gas. Further to this, as the aforementioned gas engines need to derrate power, this also implies loosing efficiency. With the alternative proposed herein those engines could be modified to increase power and efficiency to standards that cannot be seen in the industry.

Table 1
Modifications for running on APG [11].

NG engine	APG engine
Fuelled pre-chamber	Unfuelled pre-chamber
High compression ratio flat piston	Low compression ratio bowl shaped piston
Cylinder head without swirl	Cylinder head with swirl
Dry exhaust manifold	Cooled exhaust manifold
Hard Miller cycle	Otto cycle

2. Materials and methods

2.1. Test bench

This work was performed at Guascor Energy Engine's Research and Development (R&D) facility located in Vitoria-Gasteiz. The starting tests defined the physicochemical characteristics and combustion properties of the used fuel. These checks were valid for certifying fuel characteristics like methane number, lower heating value (LHV), hydrogen, nitrogen and carbon contents. These tests were performed at Guascor Energy' premises where a chromatograph is available.

The engine employed for the tests conducted during this study was a single cylinder engine which was specifically designed for developing Guascor Energy's G-86EM 2 MW engine model. The SCE which offers several benefits as compared to Multi Cylinder Engine (MCE) as shared by Oregi, I. et al. [18] is designed to simulate the combustion of the recently launched MCE version.

During the combustion process, several variables measured were recorded like ignition timing, pre-combustion period, end of main combustion, main combustion period, post-burning period, maximum rate of heat release, knocking, exhaust temperature, thermal efficiency, cylinder pressure …

The central system for controlling all the systems was the AVL PUMA system. The PUMA gathers all the data from the sensors fitted while it also acts as a master controller for all the peripherals that have their own PLCs (Programmable Logic Controller) such as the oil system, gas supply system or compressed air system.

The AVL Indicom module is a combustion measurement software which is principally employed for the measurement and analysis of the exhaust, intake and combustion chamber pressure curves. The data acquisition module utilised is the high speed Indimaster Advanced GigabitTm with 8 channels.

As for measuring components of the exhaust gases, a HORIBA MEXA 7100D exhaust gas analyser was utilised.

After defining the gas properties which are shown at the end of the present section, engine tests were carried out on the SCE test bench. Fig. 1 shows the control room of the test bench while it is monitored by the instrumentation described by Ruiz et al. [11].

It is worth mentioning that the SCE does not have a turbocharger, so the exhaust control system has to be able to simulate the back pressure caused by the turbine in a multi-cylinder engine. To achieve this effect, the test bed is equipped with two pneumatic valves in the exhaust manifold that allows the aforementioned regulation, simulating the behaviour of the turbocharger in a twelve-cylinder engine.

Using the nomenclature shown in the diagram in Fig. 2, the performance of a turbocharger system is defined according to Equation (1):

$$\eta_{Turbo} = \frac{\dot{\overline{m}}_{CYi} \bullet \Delta H_{P,Com}\left(\overline{T}_{Si}, \frac{\dot{P}_{IM}}{P_{Si}}\right)}{\dot{\overline{m}}_{CYo}} \bullet \Delta H_{P,Exp}\left(\overline{T}_{EM}, \frac{\dot{P}_{EM}}{P_{So}}\right) \quad [1]$$

where:

m = Mean mass flow (kg/s).

ΔH_p = Enthalpy of the compression (Com) and expansion (Exp) gas (J/kg).

T = Mean temperature value (K).

P = Total pressure value (bar).

Simplifying and assuming that the inlet mass in the intake manifold is the same as the outlet mass in the exhaust manifold. It is concluded that, by setting a theoretical turbo efficiency and fixing the conditions that determine the enthalpy of the compressor (intake pressure and temperature), the test bed should only control the exhaust conditions by regulating the back pressure which is done with the pneumatic valves mentioned before.

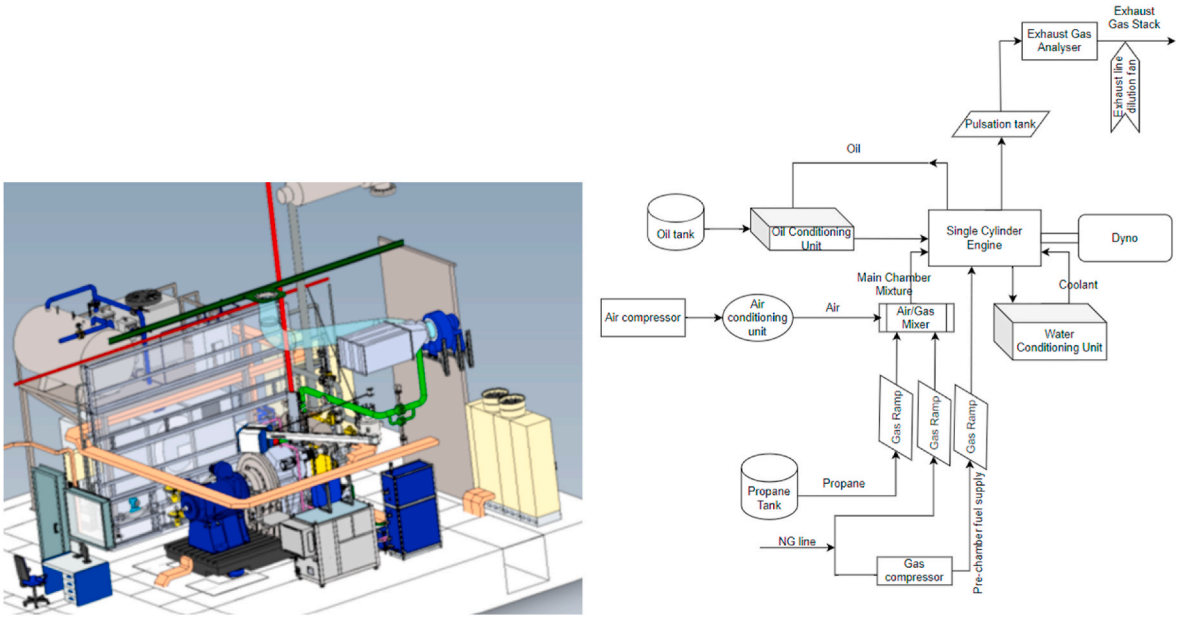

Fig. 1. SCE test bed set up.

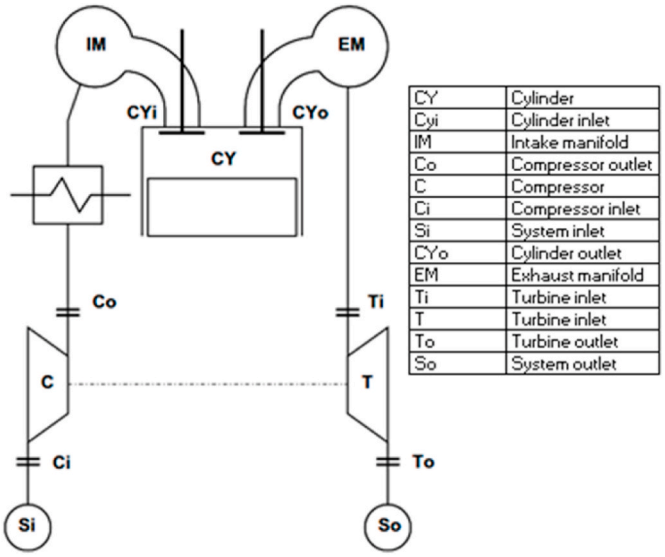

CY	Cylinder
Cyi	Cylinder inlet
IM	Intake manifold
Co	Compressor outlet
C	Compressor
Ci	Compressor inlet
Si	System inlet
CYo	Cylinder outlet
EM	Exhaust manifold
Ti	Turbine inlet
T	Turbine inlet
To	Turbine outlet
So	System outlet

Fig. 2. Schematic description of variables for calculating the performance of the turbocharger system.

2.2. Components design

In previous works, Ruiz et al. [11] explains why and how a natural gas engine with an injected pre-chamber needs to be modified to burn low methane number fuels. Taking a G-86EM from Guascor Energy as a basis, in this section, the detailed justifications about how and why **different components are designed and modified will be revealed.** It may be necessary to optimise some of the components by **testing several prototypes** of the same technology until the most suitable design is found. For a better understanding, the combustion technologies to be modified are described in the next subsections.

2.2.1. Combustion technology

A fuel injected pre-chamber ignition system requires high gas pressure (up to 6 bar) and an adjacent gas train making the system costly and presents reliability concerns due to the impurities that the APG can contain which can lead in a check valve obstruction. Since robustness and simplicity are prioritised, it is decided to use an **unfuelled pre-chamber.** This choice reduces the fuel efficiency for the same knocking margin comparing it with the previous system. The open chamber system was also an option to be evaluated for this application due to its robustness and reliability, however, the unfuelled pre-chamber possesses the following **benefits** in respect to it:

- Better fuel efficiency for the same knocking margin
- Increased combustion stability
- Lower spark plug temperature, thus, longer spark plug life
- Better economic performance for by-product fuels

It must be mentioned that if intensive work is carried out to design the geometrical parameters of the unfuelled pre-chamber the loss of efficiency mentioned in respect to the active one could be significantly reduced which enforces the decision to choose this combustion technology.

As explained by Ruiz et al. [11], the active pre-chamber, despite its higher efficiency, faces a greater susceptibility to debris and, therefore, it presents higher maintenance costs and unexpected trips. In addition, the passive chamber implies a reduction in the engine manufacturing cost. So apart from having a technical justification for selecting this system it needs to be economically justified as well.

In Fig. 3 below, the economic comparison of these two concepts with natural gas and biogas which was carried out by Lopez, A. [19]. is shown. In spite of the fact that this study aims to compare the system with biogas, the results could be transposes to APG since the price of APG is equal or even lower than biogas while the maintenance aspects for these gases are also comparable.

The left side of Fig. 3 shows, the economic comparison for natural gas between both systems with fuel price in horizontal axis and the operating hours in the vertical. As it can be observed, the active pre-chamber option is clearly the most profitable option considering that engines running on NG usually run around 7000 to 8000 operating hours per year. Thus, as per the picture it can be concluded that developing an active pre-chamber ignition system is necessary due to the high price of natural which becomes efficiency a priority.

However, on the right hand side the comparison of the pre-combustion chambers with biogas are shown. In this case, alike the APG, biogas price is subject to numerous variables, but in both cases

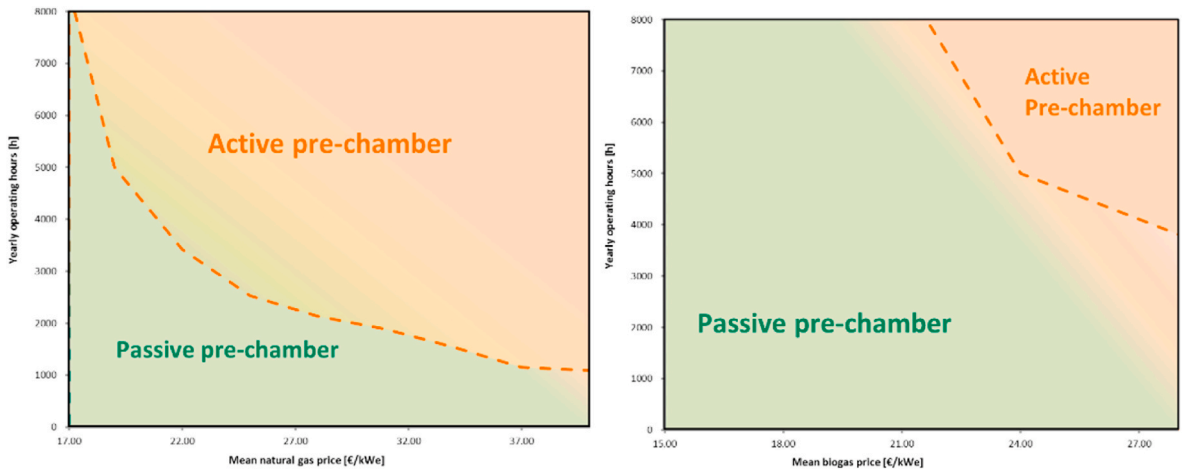

Fig. 3. Comparison of economic profitability between natural gas (left) and biogas (right) engines with active and passive pre-chambers [19].

they are considerably lower than natural gas. It is important to mention that for this calculation, maintenance costs were estimated to be higher in the passive pre-chamber due increased maintenance costs.

As a conclusion, it could be noted that an active pre-chamber for APG would only become profitable for gas prices close to those of natural gas or under very high operating hours that may not be compatible with the availability of gas in some plants. Therefore, according to this study, in addition to justifying the selection of the passive pre-chamber for technical reasons done by Ruiz et al. [11], Lopez, A. [19]. shows from an economic perspective that using an injected pre-chamber in biogas applications, and consequently in APG engines, is not sustainable.

After this modification, the engine layout remains similar to the initial one. However, the pre-chamber fuel supply line is eliminated since the new pre-chamber will only be fed with the charge that enters in the main combustion chamber via the intake valves during the intake stroke.

It must be taken into consideration that the usage of this new system entails difficulty in the load exchange process of the pre-chamber. In the fuel injected system, part of the combustion gases inside the pre-chamber were evacuated during the exhaust stroke and the rest were evacuated after the fuel injection in the pre-chamber during the intake stroke. It is known that this last stage does not exist anymore with the unfuelled pre-chamber settings and makes the charge renovation of the pre-chamber more challenging.

This trouble is tackled by an adjustment of the spark plug insertion inside the pre-chamber towards the main combustion chamber. In this way, the renovation is eased during the compression stroke since the mixture arrives faster at the spark plug position displacing the remaining combustion gases and making it easier to ignite the mixture. Furthermore, the turbulence of the charge would also help the charge renovation which is why the internal shape, nozzle diameter and nozzle orientation are modified. In fact, the pre-chamber volume is also reduced which makes it even easier to renovate it. The pre-chamber that was used during these tests is visible in Fig. 4.

The unfuelled pre-chamber presents more challenges. In the injected pre-chamber engine, it is not necessary to generate turbulence inside the combustion chamber since the high velocity torches coming from the fuelled pre-chamber are able to burn all the charge efficiently and achieve around a 100 mm fire radius. Nonetheless, if the previous turbulence levels are maintained with the new unfuelled pre-chamber, apart from the previously mentioned renovation issues the combustion would probably be incomplete and inefficient (it is estimated that the new fire radius would be 20 mm). This phenomenon is justified by the reduction of energy inside the pre-chamber mainly affected by the average lambda in the pre-chamber and its volume. That is why swirl and squish must be increased inside the combustion chamber by modifying the design of the cylinder head and piston.

The intensity and structure of in-cylinder turbulence are known to have a significant effect on performance. Changes in flow structure and turbulence intensity result in changes to the rate of heat release, cylinder wall heat rejection, and cycle-to-cycle combustion variability.

It was found that increasing the turbulence could lead to all of these [16]:

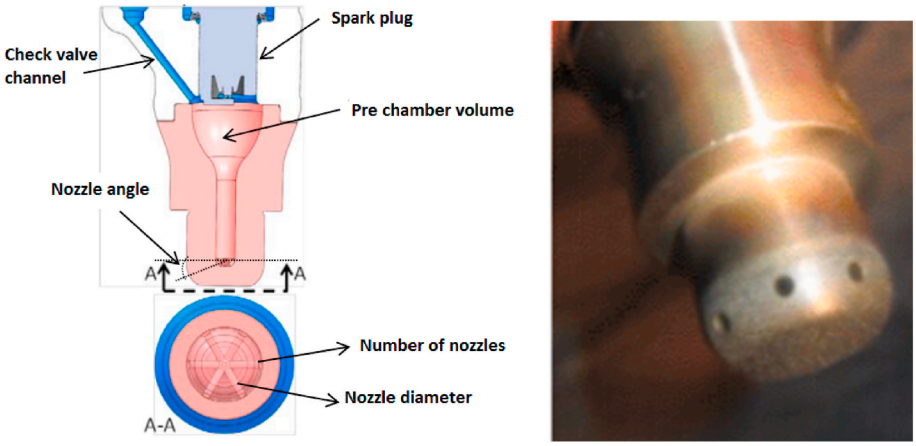

Fig. 4. Used unfuelled pre-chamber (right) and drawing (left).

- Accelerates combustion rates and reduces cyclic variability.
- Increasing in-cylinder turbulence yields lower exhaust port temperatures due to shorter burn durations and increased wall heat transfer.
- Increasing pre-chamber jet energy or squish velocity consistently results in combustion enhancement.
- The lean stability limit and the resulting minimum NO_x (Nitrogen Oxides) emission level are extended by increasing squish due to accelerated burn rate and reduced cyclic variability.
- Reductions in COV (Coefficient of Variation) of peak cylinder pressure by increasing swirl or squish can improve detonation margin.
- Increasing pre-chamber jet energy or swirl flow results in increased engine heat rejection.

Thus, in order to achieve good performance with an unfuelled pre-chamber, in-cylinder swirl and squish need to be increased.

2.2.2. Piston

2.2.2.1. Compression ratio (CR). Several manufacturers, in the attempt to burn APG using gas-piston engines, decrease the compression ratio so that the risks concerning detonations are reduced. Ruiz et al. [11] already shown in their study that 2 MW ICE with an injected pre-chamber suffered a 53.3% output power reduction when burning low methane number fuels. This scenario is not viable from a cost perspective as the €/kW of the engine is doubled. Further to this, the BMEP reduction is the main driver for experiencing a 15% efficiency drop which is something unacceptable for the market needs. For those reasons, a solution will be proposed in the following paragraphs.

It is known that if CR is reduced it will be possible to increase power maintaining the knocking margin and finally increasing the €/kW ratio. This principle is particularly interesting for the current application and therefore it is proposed to reduce the CR to solve the detonation problems posed by the low methane number of the APG.

As far as the compression ratio is concerned, it makes reference to the relation between the volume of the cylinder when the piston occupies the bottom dead centre (BDC) and the one when it is in the top dead centre (TDC) position. Thus, a higher compression ratio implies a higher pressure of the charge in the compression stroke which results in a higher pressure on the piston when the combustion begins.

For instance, according to Arutyunov [20], in the case of a Waukesha engine (VHP9500GSI) with a nominal output power of 1250 kW, the APG model suffers a reduction in the compression ratio from 10.5 to 8.0 which enables to burn fuels with MN 36.

This value was taken as a reference and the compression ratio was reduced from 13.5 to 9.1. This was achieved by changing the shape of the piston, and converting the flat piston into a bowl piston (Fig. 5). However, it was not possible to reduce the CR any further as the wall thickness of the bowl bottom part did not allow to do so.

Obviously, changing this parameter will have some effects on the engine apart from the loss of power and efficiency. Therefore, further modifications will have to be made in the exhaust manifold and camshaft because of the CR reduction.

2.2.2.2. Piston squish. In-cylinder squish needs to be increased as a consequence of selecting an unfuelled pre-chamber. Squish is defined as the motion of charge from the outer edges of the cylinder bore in towards the axis of the cylinder [16]. Discordant to the swirl, which is present all through the combustion stroke, squish flow only appears when the piston is reaching the TDC and it is rapidly decomposed into turbulent eddies as it converges at the cylinder axis. The generated squish velocity is given by equation (2).

$$v_{sq} = S_p \bullet \frac{D_B}{4z} \bullet \left[\left(\frac{B}{D_B} \right)^2 - 1 \right] \bullet \frac{V_b}{A_c \bullet z + V_b} \quad [2]$$

where:

vsq = squish velocity (mm/s);
Sp = instantaneous piston speed (mm/s);
DB = bowl diameter (mm);
Vb = bowl volume (mm^3);
z = distance between the piston crown top and the cylinder head (mm);
Ac = cross sectional area of the cylinder (mm^2);
B = bore diameter (mm).

The flat top piston used in the natural gas version is considered to be a zero squish piston, whereas pistons with squish have generally bowl geometries. If high squish velocities are needed it can be achieved by reducing the top bowl diameter, however it requires a deeper bowl to maintain the compression ratio constant. This bowl deepness cannot be reduced as much as desired, since piston thickness must be enough to support the temperatures and pressures reached in the combustion chamber. Thus, CR is limited to the piston thickness and exhaust temperature (see section 2.4).

Breaux et al. [16] exhibit the difference between a low and high squish piston obtained by the modification of the piston bowl geometry (top bowl diameter). Both bowled pistons have the same piston to head clearance.

The new piston with squish used for the experimentation can be seen in Fig. 5. This piston is adapted for the current requirements finding a compromise between a low CR and a high squish even if it has not been fully optimised for the current application. The optimisation would require the testing of different piston models.

2.2.3. Cylinder head

In order to achieve a desirable efficiency with the selected ignition

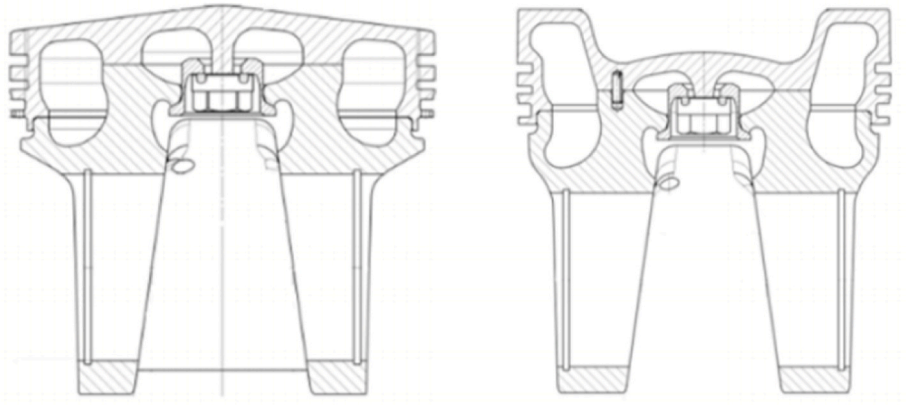

Fig. 5. Flat (left) vs crown (right) piston.

technology, it is necessary to increase in-cylinder swirl. Swirl is defined as the bulk rotation of the charge around the cylinder axis. Swirl is generated by the flow of the charge during intake and can be achieved through tangential injection of the intake charge, implementation of a swirled port geometry or by partially masking or shrouding the flow at one of the valve seats [16].

The swirl will typically persist throughout the compression and expansion stroke, gradually disappearing as a consequence of friction losses. Swirl ratio characterises bulk air motion and is defined by equation (3), as the ratio of the angular velocity of the inlet charge at the end of the induction period to the angular velocity of the engine crankshaft (swirl ratio is independent of engine speed).

$$R_S = \frac{\omega_S}{2 \bullet \pi \bullet N} \quad [3]$$

where:

Rs = swirl ratio;

ωs = angular velocity of a solid body rotating flow (rad/s);

N = engine speed (rad/s).

Increasing swirl or squish usually increments the Turbulent Kinetic Energy (TKE) of the charge [21]. This augmentation allows flow structures to last longer before their complete disappearance or permits their energy into turbulence on a smaller length scale.

It has also been confirmed that a higher swirl reduces the mean turbulent length scale within the cylinder as well as it reduces the cyclic fluctuations of the mean velocity [22]. Additionally, it has been verified that swirl converts turbulence intensity in the combustion chamber more homogenous [23] which at the same time could diminish the engine cycle-to-cycle variability. Cycle-to-cycle variability can derive to inadequate engine performance and is commonly a considerable impediment to expanding the operating range of the engine.

Due to the exposed need for increasing swirl, crescents and port shrouds will be employed in order to reach the swirl targets of 2.20 Rs (±0.10Rs). These values were selected by taking the Siemens Energy H series cylinder heads as a reference as it is a gas engine running with an unfuelled pre-chamber.

It is noteworthy that swirl cannot be augmented until infinite values in order to get higher efficiencies. A compromised balance of swirl must be found since increasing swirl produces a loss of volumetric efficiency due to the restriction (shroud) found in the cylinder head intake, as well as a higher heat transfer towards the cylinder liner which lowers the thermal efficiency. Several tests concerning swirl ratio were performed in a flow bench with the configuration presented in Fig. 6.

Upon completion of a baseline assessment concerning the initial swirl, it was determined that the original ports were highly efficient as they showed 0.06 Rs values. Afterwards, swirl crescents were designed and port shrouds were tested to reach the swirl target of 2.20 Rs (±0.10Rs).

The cylinder head was tested on the steady state flow bench using an impulse type swirl meter to measure air motion and a swirl ratio of 1.23 Rs was achieved. This was achieved by using 2 swirl crescents (increased the swirl to 0.23Rs) and using a 74% (open area) shroud.

A sensitivity study shown in Table 2 was also performed by rotating the shroud either way by a few positions (positions are every 5°) until the swirl ratio falls outside of the target range.

The 2.19 Rs position (−3) was picked despite a swirl ratio of 2.23Rs was achieved at the next position (−3). The (−2) position was felt to be more desirable as it allows a bigger tolerance on swirl crescent location and would be more robust in manufacturing.

Fig. 7 shows the seats, shroud and positions used.

The final offset crescents used had a 45-degree chamfer with a 3 mm offset. Whereas the chamfer positions were selected to be 130° for the left port and 50° for the right port.

As exposed before, position (−2) was preferred in detriment to position (−3) with a 74% open area shroud. The shroud was installed in just one port. The final shroud design is visible in Fig. 8.

Once the cylinder head was according to project needs subsequent technologies were defined.

2.2.4. Exhaust manifold

The main reason to replace the dry exhaust manifold with a cooled exhaust manifold is that the exhaust temperatures considerably rise due to various factors. Firstly, as the CR decreases, the exhaust temperature rises to levels that the material cannot tolerate. This event mainly appears because of the following:

- When the compression ratio is reduced, the expansion ratio is also reduced. The gas has a smaller expansion and therefore it has less time to cool down during the expansion.

Table 2
Swirl ratio depending on the shroud position.

Position	Swirl ratio
0	2.11
−1	2.17
−2	2.19
−3	2.23
−4	2.09
−5	2.07

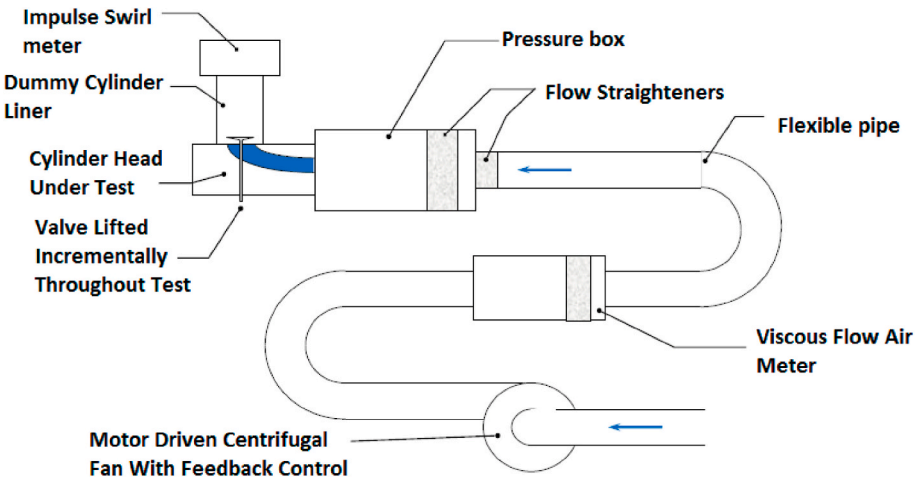

Fig. 6. Flow and swirl schematic measurement test rig.

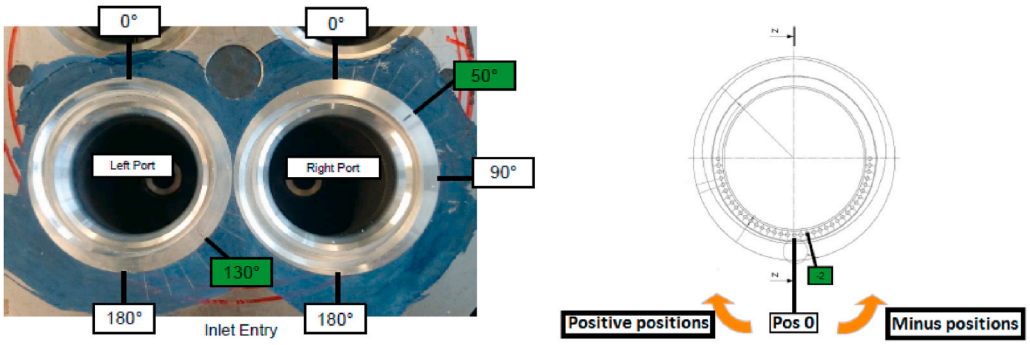

Fig. 7. Crescent (left) and shroud (right) position.

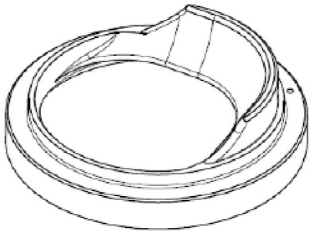

Fig. 8. Final shroud design.

- Lambda tends to be richer when the CR is reduced. Then, the richer the lambda, the higher the temperature in the cylinder and the exhaust.

If the CR is reduced the efficiency drops and that means that less energy is used in the cylinder (less expansion) and more energy is wasted in the exhaust reflecting higher temperatures/energy.

Finally, it is important to state that it is always more reliable and safe to operate at lower temperatures. However, water cooled exhaust manifold reduces the temperature at the turbine inlet and therefore the boost in the intake manifold is lower. Because of this fact, the valve timing profile needs to be carefully defined.

2.2.5. *Valve lift profile*

The G-86EM is designed to get high efficiency values and therefore operates with an advanced Miller cycle which requires a high efficiency turbocharger. However, this approach is no longer valid since some of the component modifications performed to burn low methane number gas have a big impact on the turbocharger performance.

The shrouds installed on the intake ports reduce the engine volumetric efficiency whereas the water cooled exhaust manifold reduces the amount of enthalpy available on the turbine inlet. The sum of both facts requires the installation of a highly efficient turbocharger which would lead to an increase in the engine cost. Furthermore, high efficiency turbochargers are more complex and may affect engine operation range and operation availability.

To avoid the use of sophisticated and expensive turbocharging systems, it is proposed to modify the lift of the inlet valve lift. The main goal of this modification is to increase the volumetric efficiency and thus reduce the requirements of the turbocharger.

In order to explain how a simpler turbocharger can be selected by changing the intake valve lift profile, a brief theoretical overview of both cycles must be done.

In the Miller cycle, the intake valves are closed way before the Otto cycle, permitting the charge to expand and refrigerate [24]. As a result, the mixture temperature at the compression stroke TDC is lower which allows to advance the combustion and increases the thermodynamic engine efficiency [25].

The modification of conventional Otto engines for operation on a Miller cycle can be achieved by advancing the closing of the inlet valves (EIVC), thereby limiting the amount of fresh charge that will flow into the cylinder; by delaying the closing (LIVC) so that a part of the inlet charge is rejected.

The G-86EM uses the EIVC technique for applying the Miller cycle. If the base cam valve lift profile is taken as the reference lift profile for the Otto cycle and the *EIVC Cam* is the representative for the Miller cycle. The Miller cycle the surface below the valve lift is smaller and thus a bigger pressure is needed to feed the engine [26]. This pressure must be obtained via a turbocharger with a higher compression ratio and higher efficiency.

Higher boost pressure and lower exhaust temperature are demanding conditions for a turbocharger, so an Otto cycle is chosen. It requires a lower compression ratio of the turbocharger and therefore a simpler, cheaper and more robust turbocharger can be used.

In contrast, the usage of an Otto cycle will increase the knocking tendency of the engine and the power output may need to be slightly decreased to avoid knocking issues.

Once the detailed designs of an *APG engine* have been clarified, the results of the tests conducted in a SCE will be shown in the following section. Nevertheless, it is important to underline that this is not a definitive configuration; thus, it will have to be validated after several tests and further optimisation may be needed as described in Fig. 9. However, the first approach includes the following parts that from now on they will be called the APG engine configuration:

2.1 Combustion technology: Unfuelled pre-chamber with smaller volume and higher spark plug insertion.
2.2 Piston design: Bowl shaped piston with 9.1:1 CR.
2.3 Cylinder head: 1.8 RS swirl.
2.4 Exhaust manifold: Cooled manifold.
2.5 Valve lift profile: Otto cycle.

Fig. 9 shows the experimental logic to develop the APG engine and gathers the main sources that were justified to choose and modify the NG engine combustion chamber components. The *Starting point* was covered by Ruiz et al. [11] and the main intention for this paper is to validate a first APG configuration through all the experiments that were undertaken. The optimisation of the components may be analysed in a future research.

2.3. *Test design*

In accordance with the scientific methodology, and due to the sampled data obeying a normal distribution, it is proposed to develop an analysis of the variance between the sampled variables to identify if there is a clear relation between the methane number (MN) and the thermal efficiency or peak pressure obtained. In consequence, several experiments were proposed where both variables and the NO_x emissions were sampled for a different methane number of the fuel employed in

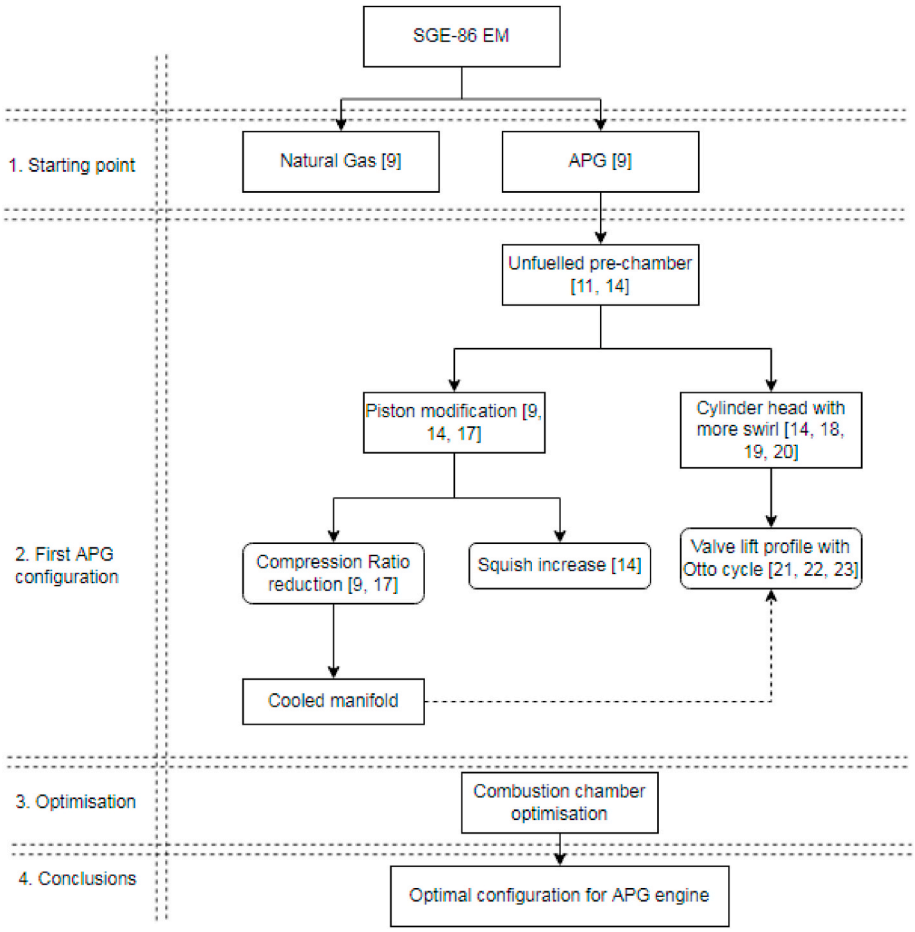

Fig. 9. APG engine design experimentation flow diagram.

each experiment.

All the tests followed the same procedure. The BMEP was increased gradually until the timing that offered the desired knocking margin (between 1500 and 2500 mg/Nm^3) was found. In order to obtain the curve, the air fuel ratio (AFR) is increased slowly starting from the lean limit (engine misfire) and finishing on the rich limit or smooth detonation area.

To be more precise, the misfire limit value, or misfire margin, will be considered as the minimum concentration of NO_x emissions (mg/Nm^3) in which the engine can work without presenting misfiring (cycles without combustion). It is a key parameter when evaluating the stability of the engine and the margin of improvement available when it comes to complying with environmental legislation on emissions. These misfiring cycles will be detected through the chamber pressure transducers and displayed on the Indimaster. The shutdown limit point will be taken as the operating point prior to the one in which the cycle without combustion is detected.

On the other hand, the knocking limit value, or detonation margin, will be considered as the maximum concentration of NO_x emissions (mg/Nm^3) in which the engine can work without detonation cycles. This is also key parameter when studying engine durability, since knocking events mechanically affect various engine components (piston, connecting rod, etc.) and engine availability. Likewise, these detonation events will be detected with the same equipment used for detecting the misfire limit and the detonation limit point will be taken as the operational point prior to the one in which the first detonation event is detected.

The ignition timing is variable and that will have to be selected before starting the tests (check section values at the end of the chapter). Priority will be given to output power instead of to efficiency. Therefore, ignition timing will be reduced as much as possible, especially for experiments 2 and 3. The limiting parameters that will not let the engine have a more retarded ignition timing are the exhaust temperature and the curve of pressure. If it is too low, the exhaust temperature will raise and COV will increase as a consequence of unstable combustion.

The results are plotted as a function of NO_x emissions which enables the direct evaluation of the effect of the configurations in the knocking margin. Even if NO_x values vary, the rest of the engine parameters are fixed except for lambda values, which means that graphics represent NO_x variations as a consequence of lambda modification. The decision to represent these curves under NO_x values instead of lambda, is justified by the fact that all current regulations make reference NO_x rather than lambda. Further to this, NO_x is a value that can be easily measured on site which provides the opportunity to compare values whereas lambda figures are complicated to measure.

As a summary, the experimental procedure will be according to Fig. 10:

It must be clarified that step 2 is only taken whenever an active prechamber is used to ignite the charge. As it will be explained in following paragraphs this will only be applicable for experiment 0 while results for that step are shown by Ruiz et al. [11] for the applicable configuration on this study. Thus, step 2 will not be discussed during the present paper.

Given the above conditions, four experiments were carried out in total:

- Experiment 0: Natural gas as a fuel and the natural gas engine configuration.
- Experiment 1: Natural gas as a fuel and APG engine configuration.

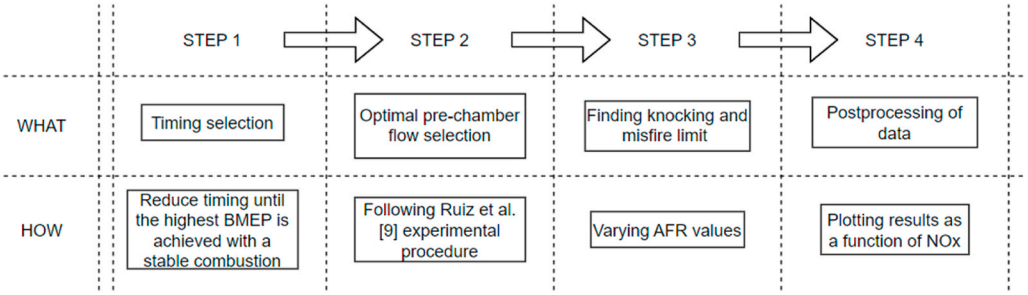

Fig. 10. APG engine design experimentation flow diagram.

- Experiment 2: A 55 NM fuel and APG engine configuration.
- Experiment 3: A 35 NM fuel and APG engine configuration.

Those four experiments were consciously selected in order to analyse two different phenomena. On the one hand, experiments 0 and 1 will exemplify the effect of all the modifications proposed in the engine. Whereas, experiments 1, 2 and 3 will show fuel's effect on the engine combustion.

Experiment 0 is considered to be the baseline against the other three experiments. Therefore, efficiency and BMEP values for this experiment will be considered a reference showing 100% values. This fact will allow a direct comparison between the new developments and the values with APG in respect of the NG counterpart which they are expected to be sensibly lower.

Table 3 gathers all the objective values for the experiments. Firstly, it must be said that for experiments 0 and 1 a lower knocking margin is selected since all the applications concerning natural gas maintain quite a stable MN during their operation. So, the risk involving gas quality variation is minimal.

The methane number MN depends on the composition of the gas and even the smallest presence of long chained hydrocarbons can lead to a drastic drop in the MN. For flare gas in particular, MN widely varies between 30 and 90 depending upon its composition [27]. This fact is related to the different qualities of oil and gas extracted in different wells around the world.

According to Williams & Filby [28], they found that the average APG MN was 68. This value was reached after a study carried out in different oil fields, while the minimum MN number appeared to be 49. However, as stated before these values could vary disproportionately depending on the countries and even the wells.

Other manufacturers' criteria for the minimal methane number acceptable is fixed typically in ~52, but they usually recommend methane numbers around 55–56 in order to ensure the correct operability of the engines [20]. During this project it was decided to go one step beyond those values designing a configuration that would be suitable for almost any APG around the world as MN35 was considered as the minimum value; having a product not only valid for wellhead gas but also for pure propane.

The boundary conditions of the experiments are as follows:

- Outlet water temperature (TWP_301): 90 °C.
- Oil temperature (TO5_001): 80 °C approx.
- Oil pressure (PO5_001): 4,5 bar.
- Inlet air temperature (TA4_001): 60 °C approx.

Table 3
Objectives for the experiments.

Experiment	Configuration	CR	MN	Knocking margin [mg/Nm^3]
0	NG engine	13.5:1	75	1500
1	APG engine	9.1:1	75	1500
2	APG engine	9.1:1	55	2000
3	APG engine	9.1:1	35	2000

- Water flow (QWP_001): 90 l/min
- Water pressure (PWP_002): 3 bar.
- Backpressure control: constant efficiency; 0.8 turbine and 0.79 compressor.
- Speed: 1200 rpm (Focused on USA market).

Variables that depend on the experiment number:

- Ignition Timing: It was adjusted in accordance with fuel knocking limits.
  - o Experiment 0: 14°BTCD (Before Top Dead Centre)
  - o Experiment 1: 26°BTDC
  - o Experiment 2: 16°BTDC
  - o Experiment 3: 14°BTDC
- BMEP: It will have to be adjusted in accordance with fuel knocking limits.

Approximate mass percentages of gas for:

- o MN75 (38,000 kJ/Nm^3)
  - Natural gas: 100%
- o MN55 (47,000 kJ/Nm^3)
  - Natural gas: 62%
  - Propane: 38%
- o MN35 (93,350 kJ/Nm^3)
  - Propane:100%

3. Results and discussion

During this section, the main sampled data obtained will be analysed and charted. Each point figures the mean of the variable during the last 60 s. In particular, experiment 0 employs 27 samples, experiment one employs 25 samples, experiment 2 employs 16 and, finally, experiment 3 employs 12 samples. To ensure repeatability and reliability of experiments more than one point has been taken per emission/lambda step and the error between those points is shown in the graphs through a standard deviation calculation.

The main goal of the present investigation is to identify the output power reduction, and thus BMEP needed to burn low methane number fuels while preserving an acceptable knocking margin (between 1500 and 2500 mgNO_xNm^3).

At the same time, the variation of the thermal efficiency in the combustion will have to be considered and studied. In order to enable an objective comparison between different configurations' influence, reference measurements were first performed on the single cylinder engine operating with the natural gas engine and natural gas. After that, the APG engine configuration proposed herein was used and evaluated for three different fuels.

As it has been already indicated, the desired detonation margin was established between 1500 NO_x and 2500 NO_x. The obtained results for the four experiments are plotted in Fig. 11 and will be subsequently analysed as specified in the experimental plan. The approximated

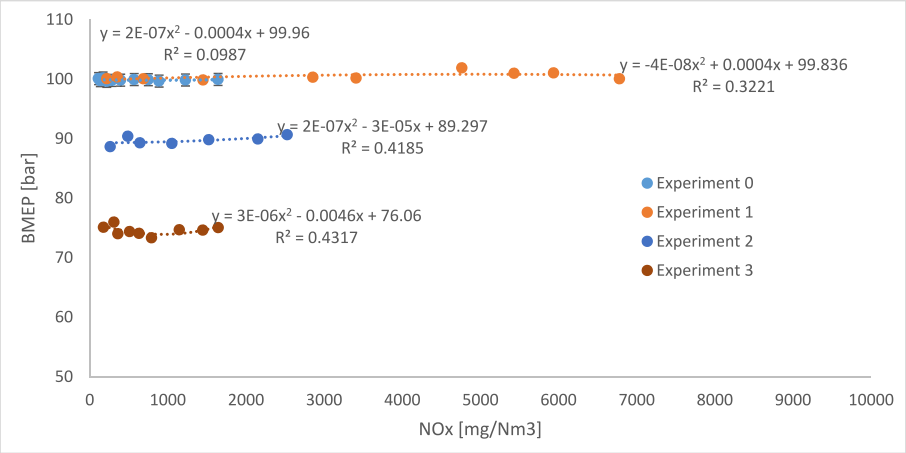

Fig. 11. BMEP vs NOx (Adequate knocking margins).

detonation margins shown in Fig. 11 are detailed in the following list.

- Experiment 0: 1600 NO_x
- Experiment 1: 6700 NO_x
- Experiment 2: 2500 NO_x
- Experiment 3: 1700 NO_x

It may be striking to consider a 6700 NO_x margin suitable for experiment 1. However, this is justified as it should be noted that the configuration of the APG engine is designed to burn low methane number fuels and it is actually burning natural gas. Therefore, the result seems logical since the initial configuration installed in experiment 0 is designed for a knocking margin of 1600 NO_x.

In spite of the fact that experiment 1 seems useless, its main objective is to show the effects of the new configuration in combustion efficiency. Obviously, in order to do that, the same experimental conditions were maintained for experiments 0 and 1, as the same fuel was used.

After having analysed the detonation margins, special focus must be put on the BMEP correlated with those margins. Finally, the BMEP results shown in Fig. 10 present the following variation percentages:

- Experiment 1: 0% reduction;
- Experiment 2: 9.56% BMEP reduction;
- Experiment 3: 25.32% BMEP reduction.

Experiment 1 suffers a 0% of variation in the BMEP comparing it with experiment 0, which makes sense since the detonation margin of this configuration is so high that the BMEP can be considerably increased without having detonation issues. Meanwhile, experiment 2 presents a 9.56% variation. However, it must be said that the knocking margin for this experiment is 2500 NO_x.

Finally, experiment 3 has a 25.32% reduction of BMEP. This value is considered acceptable considering that the MN is really low. Furthermore, the non-linear nature of the BMEP reduction must be noted. This phenomenon is related to the non-linearity inherent in the MN.

It is important to mention that with the introduced improvements the maximum output power reduction was found to be 25.32% as opposed to the original NG engine which suffered a 53.3% reduction [11]. With the aforementioned data, it can be concluded that BMEP was increased by 27.98% with the APG engine as opposed to the NG engine.

It is important to note that this fuel is under laboratory conditions, and despite having a low methane number, it obviously does not have the same composition as a field gas which may contain substances that worsen the performance but not the power output of the engine.

Subsequently, the combustion parameters between experiments 0 and 1 will be discussed. This way, multiple combustion parameters will be analysed without any effect concerning the fuel or point of operation. Thus, the effect of the components in both configurations will be understood.

As can be observed in Fig. 12, the thermal efficiency of the APG engine decreases considerably comparing it with the NG engine. In order to analyse the potential reasons for this reduction, further parameters of the combustion will have to be considered and evaluated in detail.

The respective thermal efficiency decrease of experiment 1 versus 0 is 14.05% at 500mg/Nm^{-3} NO_x. This is only used as a reference for comparison as the APG engine will be never used with natural gas, since the NG engine is specifically designed for that fuel and possesses the reference efficiency of 100%. Nevertheless, this chart indicates that there is a considerable loss of efficiency between both configurations, which has to be explained and analysed.

The main factor that makes efficiency lower is the reduction of the peak pressure. The curves of this variable for both experiments are shown in Fig. 13. Taking a look at it, it is confirmed, that the peak pressure is considerably lower in experiment 1.

This fact is completely coherent and it is mainly linked to the reduction of the compression ratio of the engine after the change of the design of the piston in order to decrease the risk of possible detonations. Among all the reasons for explaining the reduction of thermal efficiency; this one is considered to be the one with the biggest impact on efficiency reduction. It is well known that faster combustion implies a higher combustion efficiency. Considering this principle, Fig. 14 shows that experiment 0 has a much lower combustion duration, which is also closely linked to the efficiency loss shown in the previous chart.

It is verified that the combustion duration reduction is related to the usage of the APG engine components, the compression ratio has an effect on this but another major contributor is the change of the combustion system.

The fact of replacing the fuelled pre-chamber by an unfuelled pre-chamber and the reduction of its volume has a direct effect on the combustion process. The first one is able to generate a flame jet with a radius close to the liner, whereas the second system provokes a much weaker jet, which ends up in longer combustion. It has to be considered that the swirl and squish of the combustion have been increased, however, it is evident that it is still not possible to achieve the values obtained in the NG engine.

Once the compression ratio and ignition system effects have been studied, another parameter needs to be mentioned in order to evaluate the thermal efficiency properly.

Fig. 15 presents a variable that evinces the poorer performance of the new configuration. It is known that combustion is worse in experiment 1 since its exhaust temperature is considerably higher than the standard one. All of this means that higher energy is wasted and not transformed

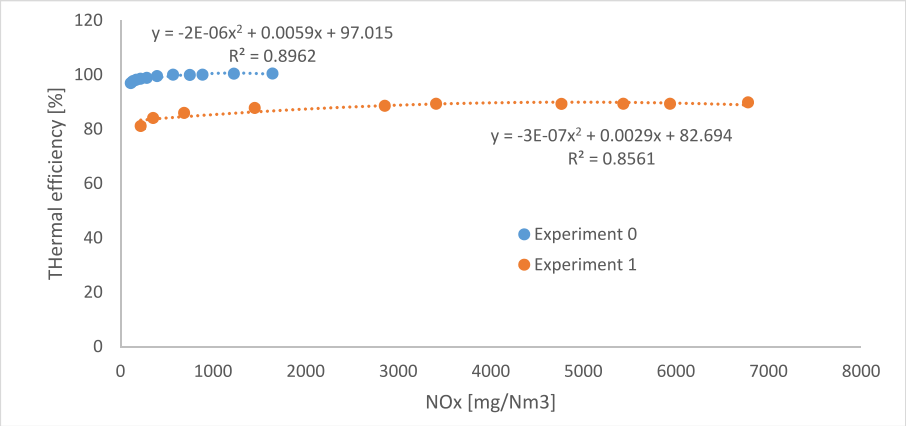

Fig. 12. Thermal efficiency vs NOx (Experiments 0 and 1).

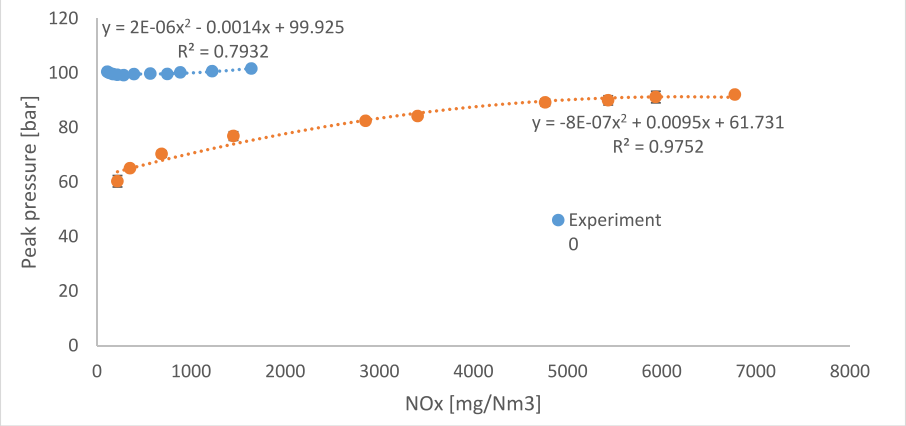

Fig. 13. Peak pressure vs NOx (Experiments 0 and 1).

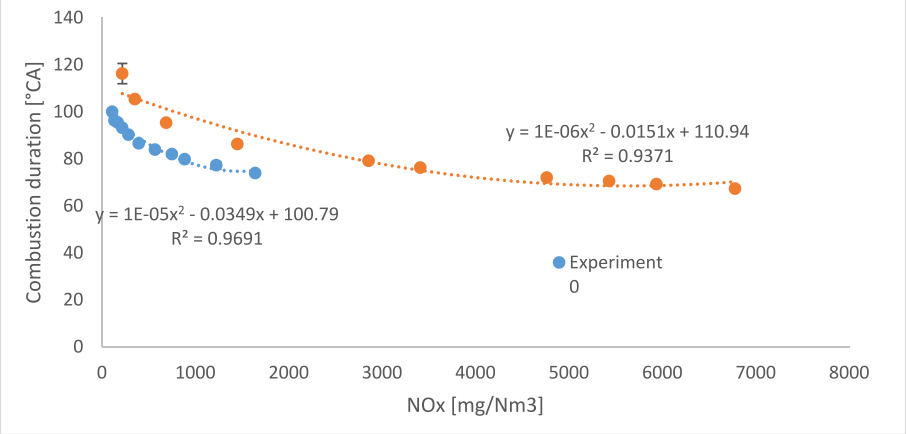

Fig. 14. Combustion duration vs NOx (Experiments 0 and 1).

into power.

Again, the main responsible for this exhaust temperature increase is the reduction of the compression ratio. When the compression ratio is reduced, the expansion ratio is also reduced. The gas has a smaller expansion and therefore it has less time to cool down during the expansion.

Nonetheless, it must be recalled that higher temperatures do present a benefit that resides in the possibility to select a wider range of turbochargers. It sounds reasonable to say that due to the high temperature, the exhaust gases possess higher energy to move the turbocharger, which will increase the boost pressure of the turbocharger (if needed) more easily.

After interpreting the influence of the different fuels in first instance, and the effects of the modification in the combustion chamber in second place, the thermal efficiency data needs to be checked. In order to do this, Fig. 16 plots the combustion efficiency of experiments 1, 2 and 3.

It is confirmed that a considerable change in efficiency exists between experiment 1 and the rest. There are two main reasons for this to

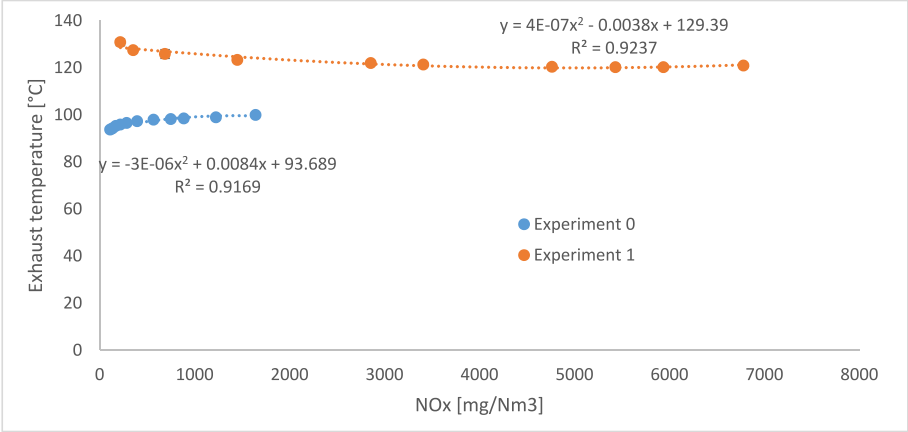

Fig. 15. Exhaust temperature vs NOx (Experiments 0 and 1).

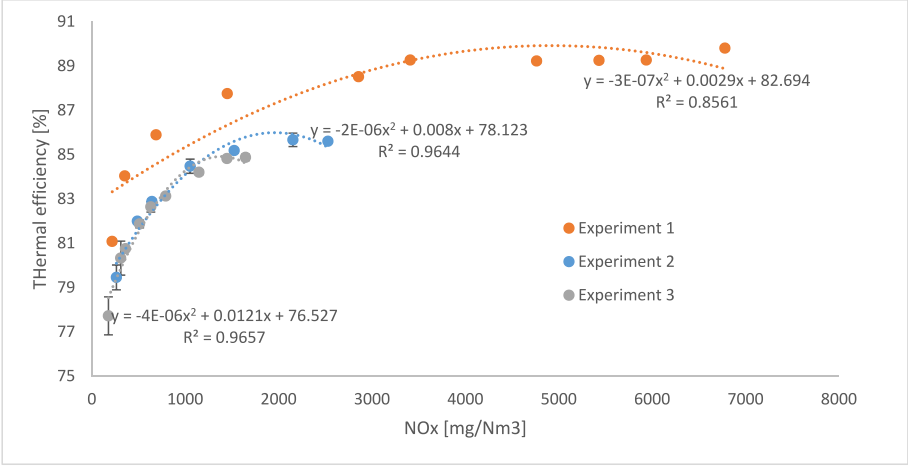

Fig. 16. Thermal efficiency vs NOx (Experiments 1, 2 and 3).

happen. The most evident one is based on the BMEP operation point. Experiment 1 is working at full load, which increases its efficiency while the other two tests are working derated, that is to say, with a power reduction. The second reason, but as important as the first one is related to the timing effect. Experiment 1 had a bigger knocking margin and therefore the timing is considerably more retarded as compared to experiments 2 and 3. The later the spark ignites the higher the efficiency will be as explained in previous paragraphs.

Nevertheless, it is noteworthy to confirm that efficiencies involving experiments 2 and 3, are reached at different BMEPs. This chart confirms that methane number mainly affects to the detonation margin and it is not one of the main players when referring to thermal efficiency drop.

The accurate percentage variations taking experiment 0 as a reference are as follows:

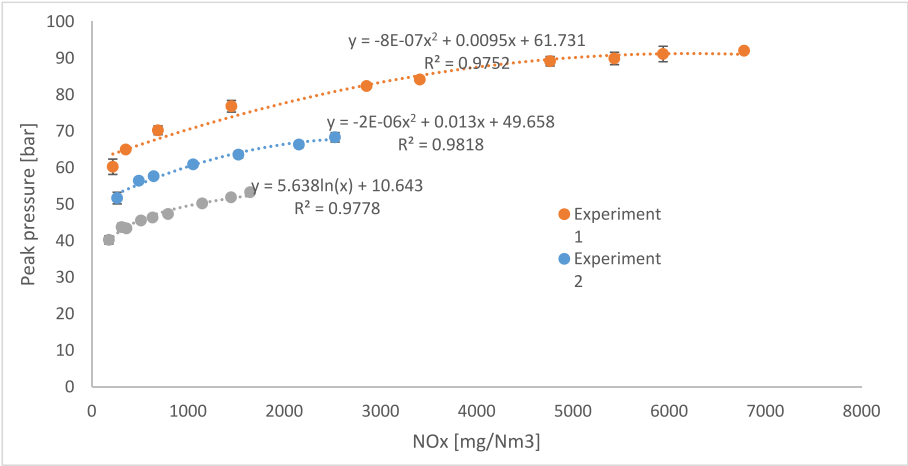

Fig. 17. Peak pressure vs NOx (Experiments 1, 2 and 3).

- Experiment 2: 17.05% reduction (Not accomplished)
- Experiment 3: 18.02% reduction (Accomplished)

As previously mentioned, the small efficiency differences between both tests could be explained by the reduction of timing and BMEP suffered in experiment 3. As it is working far from its ideal operating point the efficiency suffers a slight decrease. The plot shown in Fig. 17 supports this reasoning.

It can be contrasted that the peak pressure achieved in experiment 3 is lower than in experiment 2, thus the efficiency will also decrease. Again, the main reason why the peak pressure lowers is the reduction of the BMEP.

After the evaluation of other variables concerning combustion and its efficiencies, such as the combustion duration or the exhaust temperature; it was observed that they remain practically invariable. That is to say, the combustion with a MN 55 and a MN35 fuel is very similar except for the detonation margin.

Finally, a brief summary is included in Fig. 18 and Table 4, which graphically gathers the most important results of the investigation.

The One Way ANOVA analysis of the previous experiments showed that thermal efficiency in each experiment is independent of the methane number being the NO_x more independent than thermal efficiency from the minimum significance level of 0.05 of this study. At the same time, it was obtained a clear influence of the methane number over the peak pressure with a really high Fisher-Snedecor index, which indicates a clear influence of the MN over the peak pressure sampled for a significance level of 0.05. This same conclusion can be deduced from the previous Figs. 15 and 16. Fig. 15 shows the same tendency of the thermal efficiency versus the NO_x production for the three different methane number of the fuel employed in each test. At the same time, Fig. 16 shows three different curves of the peak pressure evolution with the NO_x production for each experiment.

Based on these results, three-dimensional models that relate the thermal efficiency and the peak pressure as a function of NO_x and methane number were obtained with an adequate determination factor for a linear model as it is shown in equations (4) and (5) and its graphical representation of Figs. 19 and 20, respectively.

$$Efficiency = 79.24 + 0.001198 \bullet NO_x + 0.0568 \bullet MN \quad [4]$$

where;

MN: Methane number.

NO_x: Nitrogen oxides production [mg/Nm^3].

Efficiency: Thermal efficiency of the process [%].

The determination factor of this model was 78%.

$$Peak\ pressure = 84.5 + 0.004695 \bullet NO_x + -0.5473 \bullet MN \quad [5]$$

where;

MN: Methane number.

NO_x: Nitrogen oxides production [mg/Nm^3].

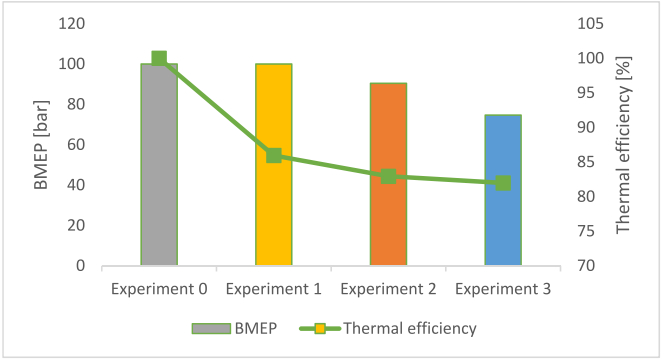

Fig. 18. BMEP and thermal efficiency (All experiments).

Table 4
Summary of experimental results.

Experiment	Experimental BMEP	Experimental Efficiency	NO_x [mg/Nm^3]
0	100.00%	100.00%	500
1	100.00%	85.95%	500
2	90.44%	82.95%	500
3	74.68%	81.98%	500

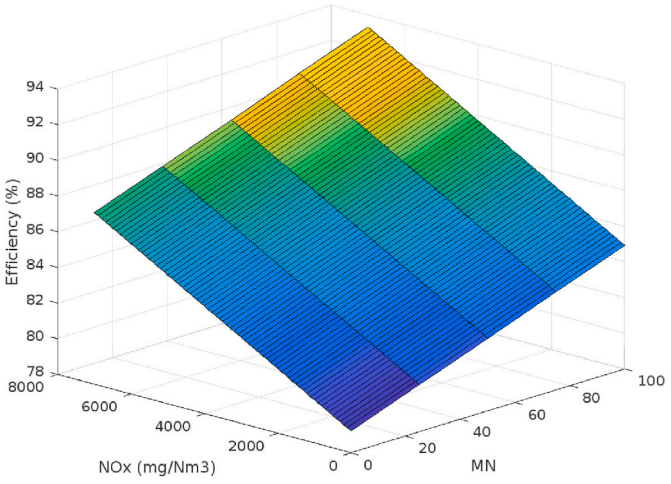

Fig. 19. Thermal efficiency versus NOx production and methane number (MN) employed.

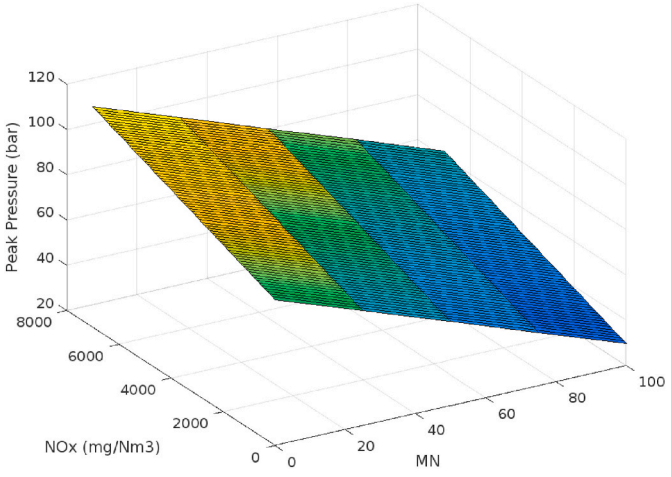

Fig. 20. Peak pressure versus NOx production and the methane number (MN) employed.

Efficiency: Thermal efficiency of the process [%].

The determination factor of this model was 97%.

From these results, it was demonstrated that the mechanical changes mainly affect the BMEP whereas, the fuel primarily affects the detonation margin and the BMEP, respectively.

The component modification with biggest impact into both, output power and efficiency is without any doubt piston's CR. As expressed above, the compression ratio is key to increase the output power and the main influence to reduce efficiency is the power drop.

In this particular study, apart from analysing experimental results as it was done along this section, comparing results with industry standards and proving the profitability of the solution becomes necessary.

It is important to remark that according to several studies derated APG engines are widely used in the industry and show profitable [7,8]

performance as a consequence of the low price of the gas. Our study herein proposes a solution that provides more power and efficiency than a derated NG engine, therefore, the viability of the solution is demonstrated as it clearly exceeds current industry standards. In fact, in terms of power loss, results were improved by 27.98% as compared to previous work results [9] showing the feasibility of this proposed technology.

Nonetheless, for having a full approach results should also be compared with other converted engines even if the used combustion technology is different. As an example, Table 5 shows the data for the same fuels for a 56SL Guascor Energy engine that fits an open chamber combustion technology.

As far as power output is concerned, the achieved experimental data in experiments 2 and 3 can be compared with Table 5. The first important topic to underline is that the 56SL reaches full power in both scenarios by reducing the CR down to 8.0:1 in the most restrictive case in line with the Waukesha VHP9500GSI engine [20]. Unfortunately, it is not possible to go below 9.1:1 on the 86 EM engine as explained in section 2.2 which are related to a piston material thickness constructive limitation. However, as compared to its NG configuration counterpart the power output with the current configuration has been increased by 27.98%, thus a 25.32% in respect to full power would be an acceptable value. Indeed, Iora et al. [1] consider power reduction of around 25% for fuels around MN45. Presents results exceed by far that figure and the power reduction with a 55MN fuel would only be a 8.56%.

As for the efficiency values, in the most restrictive scenario the engine is only 1.06% far from its counterpart. The target should be to exceed it but it can be considered as a good starting point considering that the installed configuration was a preliminary one. Likewise, comparatively it is obtained that the efficiency of an SL drops 12.47% to burn NM55 gases; whereas the EM efficiency drops 17.05%. In this case, it must be said that CR reduction in absolute numbers is bigger in the EM and therefore those results are reasonable.

In any case, results are good enough to show evidence for the adequacy of the configuration. Nevertheless, to achieve industry standards it may be necessary to carry on with the investigation through a component optimisation. This research would enable to releasing a product which offers the highest efficiency and profitability to consumers. To do so, further investigations are recommended to optimise the ignition system, meaning pre-chamber and spark plug.

4. Conclusions

From the obtained results, it was obtained that the conversion of a pre-chamber injected gas engine for burning APG with a 35MN with the proposed configuration is adequate and profitable. What is more, it was concluded that the mechanical changes mainly affect the BMEP and thus the thermal efficiency of the combustion, whereas, the fuel primarily affects the detonation margin and the BMEP, respectively. The component modification with the biggest impact on both, output power and efficiency is the piston's CR.

In addition, an outcome of this study conducted in a 175 kW single-cylinder engine (SCE) in Guascor Energy's facilities would be that the open chamber is ruled out for future developments as the efficiency still needs to be improved. The most important conclusions drawn after this experimental study are the ones related to the power and efficiency losses due to the usage of low methane number fuels taking the APG engine as a reference.

4.1. Output power

- BMEP is reduced by 9.56% using gas with MN55
- BMEP is reduced by 25.32% using gas with MN35
- BMEP and thus the power loss does not behave in a linear pattern.
- BMEP was increased by 27.98% with a MN35 fuel and the APG engine as opposed to the NG engine.

Table 5
Other engine model data.

MN	Configuration	BMEP [bar]	Efficiency @500mg/NO_x	CR
75	NG 56SL	100%	100.00%	12.3:1
55	APG 56SL	100%	87.53%	9.2:1
35	LOW APG 56SL	100%	83.04%	8.0:1

4.2. Thermal efficiency

- The efficiency drops by 17.05% when a MN55 fuel is burnt
- The efficiency reduction when using a MN35 gas amounts to 18.02%

All in all, after gathering all these results, it is concluded that the configuration proposed is adequate for burning low methane number gases. However, even the efficiency shifts to the background in the proposed application it is observed that there is still room for an ignition system optimisation as a future research work before releasing it to the market.

Credit author statement

Ander Ruiz, Iñaki Loroño, Iñigo Oregui, José A. Orosa: Conceptualization, Methodology, Software. **Ander Ruiz, José A. Orosa** Data curation, Writing- Original draft preparation. **Ander Ruiz, Iñaki Loroño, Iñigo Oregui:** Visualization, Investigation. **Iñaki Loroño, Iñigo Oregui, *José A. Orosa:*** Supervision. **Ander Ruiz, José A. Orosa**: Writing- Reviewing and Editing.

Declaration of competing interest

The authors declare that they have no known competing financial interests or personal relationships that could have appeared to influence the work reported in this paper.

Data availability

The authors do not have permission to share data.

Acknowledgements

The work presented in this contribution has been sponsored by Siemens Energy Engines R&D in the Basque Country (Vitoria-Gasteiz). The funding for open access charge: Universidade da Coruña/CISUG.

References

[1] Iora P, Bombarda P, Gómez Aláez SL, Invernizzi C, Rajabloo T, Silva P. Flare gas reduction through electricity production. Energy Sources, Part A Recovery, Util Environ Eff 2016;38(21):3116–24.
[2] Devold H. Oil and gas production handbook: an introduction to oil and gas production. second ed. ABB Oil and Gas; 2009.
[3] Vallavanatt R, Self F. Gas flare systems-last line defense. Process Saf Prog 2020;40:132e48. https://doi.org/10.1002/prs.12226. 2021.
[4] Mansoor R, Tahir M. Recent developments in natural gas flaring reduction and reformation to energy-efficient fuels: a review. Energy Fuels 2021;35:3675e714. https://doi.org/10.1021/acs.energyfuels.0c04269.
[5] Nezhadfard M, Khalili-Garakani A. Power generation as a useful option for flare gas recovery: enviroeconomic evaluation of different scenarios. Energy 2020;204:117940. https://doi.org/10.1016/j.energy.2020.117940.
[6] Morteza-Mousavi S, Lari K, Salehi G, Torabi-Azad M. Technical, economic, and environmental assessment of flare gas recovery system: a case study. Energy Sources, Part A Recovery, Util Environ Eff 2020:1–13.
[7] Chen M. Whether it is economical to use combined heat and power (CHP) system for the efficient utilization of associated petroleum gas in oil extraction sites in China: a cost-benefit analysis considering environmental benefits. Front Environ Sci, Sec. Environ Econ Manage 2022:10. https://doi.org/10.3389/fenvs.2022.984872. 2022.
[8] Vazim A, Romanyuk V, Ahmadeev K, Matveenko I. Associated petroleum gas utilization in Tomsk Oblast: energy efficiency and tax advantages. IOP Conf Ser Earth Environ Sci 2015;27:012078. https://doi.org/10.1080/15567036.2020.1737597.

[9] Jafarian H, Sattari S, Lajevardi H. Technical and economical investigation of electricity generation from associated gas. Environ Sci J Integr Environ Res 2015;4(1):33e47.
[10] Ruiz A, Loroño I, Oregui I, Orosa J. Research on an internal combustion engine with an injected pre-chamber to operate with low methane number fuels for future gas flaring reduction. Energy 2022;253. https://doi.org/10.1016/j.energy.2022.124096.
[11] Saikaly K, Le Corre O, Rahmouni C, Truffet L. Normalized knock indicator for natural gas S.I. Engines: methane number requirements prediction. 2010. p. 59e68. https://doi.org/10.1115/ICEF2009-14032. ICEF2009- 14032.
[12] Soltic P, Hilfiker T. Efficiency and raw emission benefits from hydrogen addition to methane in a Prechamber Equipped engine. Int J Hydrogen Energy 2020;45(43):23638e52. https://doi.org/10.1016/j.ijhydene.2020.06.123.
[13] Park H, Shim E, Lee J, Oh S, Kim C, Lee Y, Kang K. Large squish piston geometry and early pilot injection for high efficiency and low methane emission in natural gas-diesel dual fuel engine at higheload operations. Fuel 2022;308:122015.
[14] Singh DK, Tirkey JV. Performance optimization through response surface methodology of an integrated coal gasification and CI engine fuelled with diesel and low-grade coal-based producer gas. Energy 2022;238:121982. https://doi.org/10.1016/j.energy.2021.121982.
[15] Breaux B, Hoops C, Glewen W. The effect of in-cylinder turbulence on lean, premixed, spark ignited engine performance. Houston. In: Proceedings of the ASME 2015 internal combustion engine division fall technical conference; 2015. p. 8–11 [November].
[16] Michaut S. Market analysis for gas engine technology in Algeria. MSc. thesis, report. KTH School of Industrial Engineering and Management; 2013. Available at: https://www.diva-portal.org/smash/get/diva2:633196/FULLTEXT01.pdf.
[17] Oregi I, Garmendia E, Larralde A. Achieving best-in-clss OPEX and emissions with Siemens E-series gas engine. Electrify Europe; 2018. Accessed July 2022, https://assets.siemens-energy.com/siemens/assets/api/uuid:cf48de75-8489-42ca-ac6b-8f2dfcde85ce/paper-electrify-europe-2018-e-series-best-in-class-efficiency-lo.pdf.
[18] Lopez Martinez A. Ph.D. Thesis. Desarrollo motor de combustión interna de 2065 kW de potencia trabajando con biogás. EHU/UPV; 2020.
[19] Arutyunov VS. Utilization of associated petroleum gas via small-scale power generation. Russ J Gen Chem 2011;81(12):2557–63.
[20] Davis GC, Mikulec A, Kent JC, Tabaczynski RJ. Modeling the effect of swirl on turbulence intensity and burn rate in S.I. Engines and comparison with experiment. SAE International; 1986. SAE Technical Paper 860325.
[21] Bopp S, Vafidis C, Whitelaw JH, J.C. The effect of engine speed on the TDC flowfield in a motored reciprocating engine. SAE International; 1986. SAE Technical Paper 860023.
[22] Arcoumanis C, Bicen AF, Whitelaw JH. Squish and swirl-squish interaction in motored model engines. J Fluid Eng 1983;105(1):105–12.
[23] Coates B. Investigation of engine design parameter on the efficiency and performance of the high specific power downsized SI engine. PhD thesis. United Kingdom: Brunel University; 2012.
[24] Ribeiro B, Martins J. Direct comparison of an engine working under Otto, Miller and Diesel cycles: thermodynamic analysis and real engine performance. In: SAE International: 2007 World Congress. Detroit, Michigan; 2007. p. 16–9 [April].
[25] Li T, Gao Y, Wang J, Chen Z. The Miller cycle effects on improvement of fuel economy in a highly boosted, high compression ratio, direct-injection gasoline engine: EIVC vs. LIVC. Energy Convers Manag 2014;79:59–65.
[26] Elsenbruch T. Stop flaring and venting – utilization of APG with gas engines. 2nd M2M Partnership Expo [online] New Delhi, India, 2-5 March. 2010. Accessed July 2022, https://www.globalmethane.org/expo-docs/india10/post-expo/oil_elsenbruch.pdf.
[27] Williams S, Filby B. Rocky mountain GPA: fuel gas conditioning for remote reciprocating engines. 2013.

Definitions/Abbreviations

AFR: Air Fuel Ratio
APG: Associated Petroleum Gas
BDC: Bottom Dead Centre
BMEP: Brake Mean Effective Pressure
BTCD: Before Top Dead Centre
CHP: Combined Heat and Power
COV: Coefficient of Variation
CR: Compression Ratio
EIVC: Early Inlet Valve Closing
ICE: Internal Combustion Engine
LHV: Lower Heating Value
LIVC: Late Inlet Valve Closing
MCE: Multi Cylinder Engine
MN: Methane Number
NG: Natural Gas
R&D: Research and Development
SCE: Single Cylinder Engine
TDC: Top Dead Centre
TKE: Turbulent Kinetic Energy
UDC: University of Coruña